Institute of Paper Science and Technology
Atlanta, Georgia

IPST Technical Paper Series Number 749

Bubble Size Measurements in a Quiescent Fiber Suspension

T.J. Heindel

August 1998

Submitted to
Journal of Pulp and Paper Science

Copyright© 1998 by the Institute of Paper Science and Technology

For Members Only

INSTITUTE OF PAPER SCIENCE AND TECHNOLOGY
PURPOSE AND MISSIONS

The Institute of Paper Science and Technology is an independent graduate school, research organization, and information center for science and technology mainly concerned with manufacture and uses of pulp, paper, paperboard, and other forest products and byproducts. Established in 1929, the Institute provides research and information services to the wood, fiber, and allied industries in a unique partnership between education and business. The Institute is supported by 52 North American companies. The purpose of the Institute is fulfilled through four missions, which are:

- to provide a multidisciplinary education to students who advance the science and technology of the industry and who rise into leadership positions within the industry;
- to conduct and foster research that creates knowledge to satisfy the technological needs of the industry;
- to serve as a key global resource for the acquisition, assessment, and dissemination of industry information, providing critically important information to decision-makers at all levels of the industry; and
- to aggressively seek out technological opportunities and facilitate the transfer and implementation of those technologies in collaboration with industry partners.

ACCREDITATION

The Institute of Paper Science and Technology is accredited by the Commission on Colleges of the Southern Association of Colleges and Schools to award the Master of Science and Doctor of Philosophy degrees.

NOTICE AND DISCLAIMER

The Institute of Paper Science and Technology (IPST) has provided a high standard of professional service and has put forth its best efforts within the time and funds available for this project. The information and conclusions are advisory and are intended only for internal use by any company who may receive this report. Each company must decide for itself the best approach to solving any problems it may have and how, or whether, this reported information should be considered in its approach.

IPST does not recommend particular products, procedures, materials, or service. These are included only in the interest of completeness within a laboratory context and budgetary constraint. Actual products, procedures, materials, and services used may differ and are peculiar to the operations of each company.

In no event shall IPST or its employees and agents have any obligation or liability for damages including, but not limited to, consequential damages arising out of or in connection with any company's use of or inability to use the reported information. IPST provides no warranty or guaranty of results.

The Institute of Paper Science and Technology assures equal opportunity to all qualified persons without regard to race, color, religion, sex, national origin, age, disability, marital status, or Vietnam era veterans status in the admission to, participation in, treatment of, or employment in the programs and activities which the Institute operates.

BUBBLE SIZE MEASUREMENTS IN A QUIESCENT FIBER SUSPENSION

Theodore J. Heindel
Institute of Paper Science and Technology
500 10th Street, N.W.
Atlanta, GA 30318-5794
USA

KEYWORDS: bubble size measurement, flash x-ray radiography, flow visualization, fluid mechanics, ONP, flotation deinking

ABSTRACT

Flash x-ray radiography (FXR) is utilized to visualize rising air bubbles in an ONP fiber suspension at various fiber consistencies. In general, most air/water/fiber systems are opaque, but the FXR technique allows for bubble visualization in the bulk suspension. Images of air bubbles injected at the base of a column filled with ONP fibers at various consistencies reveal that the bubble rise characteristics and patterns are highly dependent on fiber consistency. Bubble size measurements are also obtained by image analysis of the FXR images and are shown to be influenced by both fiber consistency and air injection method.

INTRODUCTION

A greater understanding of the fluid dynamic behavior of complex three-phase fibrous systems is important to the pulp and paper industry, where gas/liquid/fiber suspensions occur in many areas. Any region where stock heating is performed by direct steam injection forms a three-phase system. For uniform and efficient heating, a homogeneous steam distribution must occur throughout the water/fiber slurry. In paper recycling, control of gas/liquid/fiber flows is important for effective flotation deinking operations. In this process, air is injected into a fibrous suspension and hydrophobic contaminant particles attach to the hydrophobic bubble surface. The resulting aggregate rises to the surface where the contaminants are removed. A bubble must be large enough to rise through the fiber network, but if the bubble is too large, channeling is promoted where the majority of the injected air rises in discrete regions, which leaves other regions deficient of air bubbles and decreases operating efficiency. Gaseous bleaching is another process where knowledge of gas bubble size is important for successful operations. A homogeneous distribution of small gas bubbles will promote uniform bleaching and minimize chemical consumption. All of these operations involve a gas/liquid/fibrous multiphase system, and all benefit from knowledge of the bubble flow characteristics and bubble size distributions in the suspension. With this knowledge, system operation can be optimized and enhanced to increase efficiency and reduce chemical and energy costs.

Measuring bubble size and recording bubble flow patterns is rather easy when the system is transparent, such as air rising through a column of water. In these situations, optical visualization and laser techniques are commonly utilized. When the system is translucent or opaque, common in many multiphase operations, optical and laser techniques can only be used near the system boundaries (i.e., walls) or when a fluid sample is redirected through a narrow region to enhance visualization. However, information gathered near the system boundaries, or from a small sample removed from the system, may not represent true operating conditions within the bulk flow. For these systems, it may be possible to insert special probes into the bulk flow to record bubble

parameters of interest. Descriptions of many measurement and visualization techniques for multiphase flows are available in the literature [1-6].

Difficulties may arise with traditional experimental tools such as high-speed video, laser velocimetry, electrical resistivity probes, or optical probes when a complex multiphase system is translucent or opaque and has one phase (typically the solid phase) that may interact with, or impede the performance of, intrusive probes. Gas/liquid/fiber suspensions, common in the pulp and paper industry, is one such multiphase system. Attempts to visualize these complex fiber suspensions have been conducted by Walmsley [7], where water was replaced by clove oil to produce a system that had the same refractive index as wood fiber. However, applicability of these results to gas/water/fiber systems is unknown. Hunold et al. [8] measured bubble size in dilute fiber systems of less than 0.5% consistency by weight by suctioning a small sample out of the test cell and passing it through a capillary tube. Intermittent gas volumes were recorded and translated to equivalent gas bubble diameters, assuming no bubble coalescence occurred in the capillary tube or suction head. Bubble size measurements have also been obtained in air/water systems to calibrate air injectors used in flotation deinking studies [9]. This information was then utilized to relate bubble size to flotation deinking performance, although the calibration was performed in the absence of fibers. However, the presence of fibers may have a significant effect on bubble coalescence and size, so actual bubble size during the flotation experiments may have changed considerably.

To capture bubble size and bubble flow characteristics in gas/water/fiber systems at consistencies typically employed in the pulp and paper industry, additional tools and/or techniques must be utilized. One such technique that can visualize gas flows in complex multiphase systems is called flash x-ray radiography (FXR). This is a process where an intense burst of x-rays is produced for a fraction of a second to record dynamic events on film that cannot be captured by conventional photography. Current areas where FXR is commonly utilized include high velocity ballistics, explosion analysis, weapons development, nondestructive testing, and medical and

biological studies [10-12]. FXR also has the ability to penetrate opaque, complex fluids and produce a permanent film record of internal gas flows [13-15]. In the pulp and paper industry, FXR has been utilized to visualize paper formation [16, 17], black liquor spray formation [18], coating applications [19], and impulse drying conditions [20]. Recently, FXR has been applied to air/water/fiber flows to observe and record the gas flow characteristics in a rectangular bubble column filled with a fiber slurry at consistencies common to flotation deinking [21, 22]. The commonality between these processes is that the events of interest are typically high speed and the region of visual interest is obscured - an ideal application for FXR.

In this study, FXR was used to visualize air flows in an ONP suspension at various fiber consistencies and air flow rates to compare and contrast these flows to air/water systems. Additionally, bubble size measurements were obtained from the FXR images and two types of air injection techniques were compared to determine if conclusions obtained in an air/water system (a much easier system to work with) were applicable to air/water/fiber systems.

EXPERIMENTAL PROCEDURES

Figure 1 is a schematic representation of the experimental setup used in this study. The x-ray unit was a 300 keV HP 43733A flash x-ray system (currently supported by Primex Physics International), which generated a 30 nanosecond x-ray pulse. The x-ray tube head was mounted in a locking vertical slide to allow x-ray exposures at various heights. A 3.25 mm thick aluminum filter was mounted directly in front of the x-ray source aperture to filter soft x-rays that promote scattering effects and result in fuzzy images [12]. The resulting hardened x-ray beam produced sharper images with less scattering.

The entire system was housed in a 3.5 m $\times$ 4.5 m room lined with lead foil for safety. A bubble column with rectangular cross section, 20 cm $\times$ 2 cm, was constructed with face panes of 6.35 mm clear acrylic stock. The column was 1 m tall with lead numbers affixed to both sides to indicate the column height. The numbers were recorded on film when x-rays were taken to identify

the column location. Compressed air was injected into the base of the column by one of two methods referred to in this study as septum or sparger, respectively.

The septum air injection method consisted of a single, centrally located hole drilled in a 3.18 mm thick n-butyl rubber plate. The hole was formed with a 0.34 mm diameter drill bit and was self-sealing when the air pressure was removed. The rubber septum separated the bubble column from a conical air diffuser and allowed for the possibility of using other septums with different air injection patterns and/or hole sizes.

The sparger air injection method utilized a sintered bronze filter commonly used to remove 40 μm particles from compressed air supplies. It was attached to the end of an air line and placed on the bottom of the column. The air line was inserted through the column top and positioned near the column wall such that it did not interrupt the bulk air flow patterns.

Air flow through the septum or sparger was regulated with a Dixon air regulator and filter, and was measured with a Sierra Instruments mass flow meter that covered an air flow rate range of less than 1 slpm (standard liter per minute). The entire bubble column was mounted on a support stand with locking wheels to allow horizontal placement from the x-ray source.

A single 20 cm × 25.2 cm x-ray negative was exposed during the discharge of the x-ray unit. The x-ray film was AGFA D8 Structurix film and was mounted in a film cassette between two Dupont Quanta Rapid Back PF intensifying screens. This was performed in a lightproof room where the x-ray negatives were also developed using standard processing procedures [23].

Each x-ray negative was exposed by attaching the film cassette to the back of the bubble column in one of four positions identified in Fig. 1, and then discharging the x-ray unit. A lead letter/number identification was taped to each cassette to permanently identify the image when exposed to radiation. The x-ray source was located in front of, and perpendicular to, the rectangular bubble column. All radiographs were taken at a source to film distance of 1.65 m and

an object to film distance of 1.6 cm, ensuring negligible image magnification and distortion [11, 12]. The bubble column and x-ray tube were aligned using a laser pointer mounted on top of the x-ray tube so that the x-ray aperture was coincident with the center of the x-ray film.

The system of interest was composed of deionized water with or without unprinted ONP (old newspaper) fibers, through which filtered building air was bubbled. The ONP was reslushed following TAPPI method T 205 om-88 [24]; however, deionized water was used, and the disintegration was performed at 1.2-1.3% consistency. Four samples from the slurry were analyzed by a Kajaani FS-100 fiber length analyzer for fiber length characterization yielding a weighted mean fiber length of 1.4 mm. Fiber slurries of 0.1, 0.5, and 1.0% consistency by weight were prepared by diluting samples of the reslushed stock with deionized water.

The bubble column was charged by filling it from the top with 3.2 L of the desired water/fiber slurry, which corresponded to a column fluid height of 80 cm. This allowed for fluid expansion in the column once air was introduced into the system. The column was drained when not in use through a valved opening located on the column side near its base. After filling, the fiber suspension slowly separated over a period of hours if the system was not agitated. Therefore, a moderate air flow rate was maintained to keep the system well mixed. After an experiment was set up and the x-ray film was properly located, the air flow rate was adjusted to 0.25 slpm, corresponding to a superficial gas velocity (air flow rate divided by the column cross-sectional area) of 0.10 cm/s. A waiting period of 10-15 minutes allowed the flow to reach quasi-steady-state conditions, whereupon an x-ray was taken.

Once the FXR images acquired in this study were developed, they were analyzed using image analysis software. Bubble areas were recorded and converted to equivalent bubble diameters, defined as the circular diameter whose area was equal to that of the bubble. A Sauter mean bubble diameter was then determined by $d_{32} \equiv \Sigma d^3/\Sigma d^2$, where the summation takes place over the entire bubble population and d is the equivalent bubble diameter. The Sauter mean is a

ratio of bubble volume to bubble surface area and is typically recorded in bubble (or drop) size experiments [5]. A smaller Sauter mean diameter indicates more surface area per unit bubble volume, a desirable characteristic in flotation and bleaching operations.

A series of four x-rays, one at each position, were obtained for each fiber consistency. These x-rays were used to explain general qualitative observations. Additional x-rays were taken at Position 2 (see Fig. 1) to gather enough bubble size measurements (more than 700 for each experimental condition) to calculate bubble size distributions. Typically, 6 to 18 additional x-rays, depending on fiber consistency, were required to obtain the desired bubble population sample.

Verification of the ability of the FXR technique to capture a true image of air bubbles rising through water was completed by Monefeldt [23] by comparing images acquired with high-speed video photography with those obtained at the same time (± 0.033 sec) using FXR. The same bubble column used in this study was used in [23], but with multiple air injection holes. Very good qualitative agreement was obtained, and the same bubbles and bubble groups were identified on both the video and FXR images.

RESULTS

Flash x-rays of an air/water system (0% consistency) and an air/water/ONP fiber system at 0.1, 0.5, and 1.0% consistency by weight were obtained at four locations in a rectangular bubble column for a fixed air flow rate of 0.25 slpm, corresponding to a superficial gas velocity of 0.10 cm/s. Two different air injection techniques were studied in this investigation. No additional system chemistry (i.e., soaps, collectors, etc.) was added to the suspension during the tests. FXR and high-speed video photography bubble size distributions in an air/water system will first be compared to verify the utility of the FXR technique. Then qualitative observations between an air/water system and the air/water/fiber system will be presented. Finally, bubble size distribution measurements will be summarized for two different air injection techniques and various fiber consistencies.

Bubble Size Measurements with FXR

X-rays and high-speed video were taken with the septum air injection technique in an air/water system with a fixed superficial gas velocity of 0.10 cm/s. Using image analysis, bubble size measurements were obtained at Position 2, resulting in a Sauter mean diameter of 5.0 and 3.6 mm, respectively, for the high-speed video and x-ray images. Under identical experimental conditions, the video analysis results in a larger Sauter mean bubble diameter than that recorded with the FXR technique. The corresponding bubble size distributions for this air/water system are shown in Fig. 2. The general shape of the bubble size distributions are similar, but the distribution obtained from the video images show a shift to larger bubble diameters when compared to the FXR images.

The reason for the discrepancy in recorded bubble diameter distributions between the two imaging techniques, with identical experimental conditions, is described in Fig. 3. In the high-speed video analysis, the high intensity light used to record the bubble images is reflected off the bubble surface and recorded on the video film as a sharp contrast between the air bubble and fluid medium interface (Fig. 3a). The resulting high contrast at the bubble/fluid interface is ideal for image analysis. In comparison, the amount of x-rays transmitted (or absorbed) and eventually incident on the x-ray film is a function of the depth of material through which the x-rays pass. The amount of x-rays transmitted along a chord passing near the bubble periphery is less than the amount transmitted along a chord through the bubble center because the x-rays pass through more water near the bubble periphery, and water absorbs approximately 1000 times more x-rays than air. This results in a gray-scale variation from the bubble center (a very dark region because more x-rays pass through this region) to the bubble edge (a lighter region because more x-rays are adsorbed by the water). Upon image analysis, this produces a loss of bubble projected area onto the film due to lack of image contrast at the bubble/fluid interface (Fig. 3b).

Hence, actual equivalent bubble diameters are difficult to recorded with the current experimental facility. However, relative bubble sizes can be determined and compared to those

obtained with differing experimental conditions. For example, FXR can be used to determine if bubbles are larger or smaller when one system parameter, such as fiber consistency, is varied.

Quantitative Comparisons Between Air/Water and Air/Water/Fiber Flows

Figure 4 shows the composite of the four x-ray images taken of a water column with air injection (0% consistency). Each image was taken at a separate time interval, and the figure represents a composite of the conditions at each column position. The gap between the channel bottom where air is introduced and the beginning of the first image is due to the flange and bolts that are used to attach the column to the air diffuser, preventing the film cassette from being placed any lower. The gaps between Positions 1 and 2, Positions 2 and 3, and Positions 3 and 4 are caused by the film cassette holder being fixed at specific column locations. The actual image dimensions that encompass the column interior are 20 cm × 20 cm with approximately 2.5 cm of film overhanging each side. The overhanging portions include the lead position indicators and radiograph identification labels, and have been digitally removed from the images presented here to increase clarity. The digitized and reduced images do have some loss of detail, but the images are representative of the originals. Similar loss of detail was highlighted by Rowe and Partridge [15]. In this study, all observations are based on the original x-ray negatives, which are available at the Institute of Paper Science and Technology.

Air was introduced through the septum from a central location at the column base, as indicated in Fig. 4. The small dark dots represent air bubbles as they rise through the column (Fig. 4a). The air bubbles rise in a serpentine pattern and become well dispersed toward the top of the water column, as highlighted in the schematic representation of the bubble rise region (Fig. 4b). Figure 5a displays a close-up of one of the Position 2 x-rays and encompasses a region 8.8 cm × 6.7 cm. The air bubbles, represented by the dark regions, are actually oblate spheroids but appear on film as ellipses with the major axis oriented horizontally. Figure 5b shows the digitized outline of the bubbles obtained with the image analysis software, emphasizing the general elliptical shape.

Adding fibers to water results in an increase in the effective viscosity, compared to pure water [25]. The corresponding increase in viscous drag results in slower bubble rise velocities and smaller bubble Reynolds numbers. When as little as 0.1% consistency by weight of cellulose fiber is added to the system, the bubble shape changes from generally oblate spheroid to more spherical, but the serpentine flow pattern still exists. The general shape changes are revealed by comparing Figs. 5a,b with Figs. 5c,d. The change in bubble shape to more spherical when fiber is added to the system will also decrease the bubble surface area.

The serpentine flow pattern is altered when the fiber consistency increases to 0.5%, a consistency at which fiber networks are known to form [26]. Figure 6 reveals the flow pattern for 1% fiber consistency (a common consistency encountered in flotation deinking), which is very similar to that observed at 0.5% consistency. This composite x-ray image (Fig. 6a), and the accompanying schematic representation (Fig. 6b), clearly show the flow pattern differences from those observed in the air/water system. The bubbles in the original x-rays reveal a shape that is more spherical than the bubbles observed in the pure water situation. The fiber networks that form at consistencies greater than 0.5% can impede bubble rise and trap bubbles that do not have a sufficient buoyant force to break through. Other bubbles may eventually coalesce with the trapped bubbles and provide the required buoyant force to break though the network. In addition, the increase in network formation and the relative high effective viscosity impairs bubble dispersion, and the rising air bubbles remain in a confined region. Similar observations were recorded by Iguchi et al. [27], who investigated the effect of liquid viscosity on the behavior of a rising bubbling jet in a cylindrical vessel filled with an aqueous glycerol solution. The air bubble confinement is the beginning of channeling for the fluid system of this study, a phenomenon where air bubbles rise in some regions and not in others. Channeling can lead to a significant reduction in gas/fluid interfacial area and degrade system performance.

Although the sparger air injection method differs considerably from the septum air injection method, the overall bubble flow patterns observed at the various fiber consistencies remains similar.

Bubble Size Measurements in Air/Water/Fiber Flows

Bubble size measurements were obtained from the x-rays taken at Position 2 for systems with 0, 0.1, 0.5, and 1.0% ONP consistency by weight. Bubble size distributions were obtained from these measurements with at least 700 bubbles making up each bubble population sample. This typically required 6 to 18 x-rays to be taken of Position 2 with the desired experimental conditions. More x-rays were required as the fiber consistency increased. General conclusions from these measurements are summarized in Table 1.

In an air/water system, the sparger air injection method produces more and smaller bubbles than the septum air injection method, resulting in a sparger average bubble size of 2.0 mm compared to the septum average bubble size of 2.9 mm. Therefore, bubble size measurements performed in water reveal that the 40 μm sparger used in this study will produce smaller bubbles than the septum with a single hole made with a 0.34 mm diameter drill bit. A similar trend is observed in the 0.1% fiber consistency system. However, the average equivalent bubble size does increase slightly when the consistency increases from 0 to 0.1% (see Table 1).

When the fiber consistency increases to 0.5%, a significant change occurs in the bubble dynamics to yield a new trend, resulting in the septum air injection method now producing the smaller average bubble size. This new trend continues at a consistency of 1%. With the septum now producing bubbles with a smaller average equivalent diameter at Position 2 than the sparger, the conclusions obtained in the air/water system (0% consistency) are not in agreement with those observed in the air/water/ONP system at 0.5 and 1% consistency.

The change in bubble size distribution as the consistency increases is shown in Fig. 7 for the septum air injection technique. When the septum is used to introduce air into the system, the

bubble size distribution does not change considerably until the consistency reaches 1%. Then the bubble size distribution shifts slightly to larger equivalent diameters. The sparger air injection technique does not reveal the same trend (Fig. 8); increasing the consistency results in a broader bubble size distribution, with the mean value shifting to larger diameters.

These differences can be explained by how the bubbles leave the region where they are introduced into the system. Increasing the fiber consistency increases the network formation within the system, which slows the bubble ascension. The septum produces relatively large air bubbles in water. The bubbles have a sufficient buoyant force to be removed as soon as they form at the septum air inlet. The buoyant force associated with these relatively large bubble sizes is sufficient to break through the fiber network, even for fiber consistencies as high as 0.5%. At 1% consistency, the fiber network is such that the bubbles are slowed enough so they coalesce to form larger bubbles as they rise. The resulting larger bubbles have an increased buoyant force to rise through the fiber network.

In contrast, the sparger produces very small bubbles in water, and they all enter the system in a small region around the sparger head. These bubbles quickly disperse in water to limit any bubble coalescence that may take place. When the fiber consistency increases, particularly to 0.5%, the small bubbles no longer have a sufficient buoyant force to rise through the fiber network. Hence, the small bubbles coalesce upon introduction into the system to form larger bubbles with a sufficient buoyant force to break through the fiber network. Further increases in the fiber consistency increase the bubble size slightly to form yet larger bubbles. This is revealed by a high frequency of large bubbles when the sparger is used.

The effect fiber consistency has on the Sauter mean bubble diameter is summarized in Fig. 9. Increasing the consistency results in an increase in the Sauter mean bubble diameter. These increases are on the order of 0.5 and 2.0 mm for the septum and sparger air injection technique, respectively, when the fiber consistency is increased from 0 to 1%. The significant conclusion from this figure is that the air injection technique can have a substantial influence on the Sauter

mean bubble diameter and, as shown in Figs. 7 and 8, on the equivalent bubble size distribution. Furthermore, the conclusions drawn at 0% consistency (i.e., a simple air/water system) are not the same conclusions found when ONP fiber is added to the system.

CONCLUSIONS

Flash x-ray radiography (FXR) was a useful tool for visualizing gas bubbles in an opaque fibrous suspension. Images of air bubbles injected at the base of a column filled with ONP fibers at various consistencies revealed that the bubble rise characteristics and patterns were dependent on fiber consistency. Air bubbles became larger, less dispersed, and followed preferential rise paths as the fiber consistency increased. Bubble size measurements were also obtained from the x-ray images and were shown to be influenced by both fiber consistency and air injection method.

The most important outcome from this study was that conclusions for different air injection methods obtained in an air/water system may not be applicable to opaque fibrous slurries. Specifically, it was shown that the sparger air injection technique used in this study produced smaller air bubbles than the septum air injection technique in an air/water system. However, at 0.5 and 1% ONP fiber by weight, the opposite trend occurred, and the septum air injection technique was shown to produce smaller bubbles. Therefore, generalizations made in simple multiphase systems that allow easy visual access should be applied with caution to complex fibrous multiphase flows.

ACKNOWLEDGMENTS

The work described in this paper was funded by the Member Companies of the Institute of Paper Science and Technology. Their continued support is gratefully acknowledged. Special thanks are extended to Ms. Adele Emery for shooting and developing all of the x-rays presented here and performing all of the bubble size measurements. Mr. Paul Phelan is also recognized for his FXR training and troubleshooting expertise. Additionally, the help of Mr. James Monefeldt in formalizing some of the FXR procedures used in this study is gratefully acknowledged.

REFERENCES

1. CLIFT, R., GRACE, J.R., and WEBER, M.E., "Bubble, Drops, and Particles", Academic Press, New York (1978).

2. HETSRONI, G., Ed. "Handbook of Multiphase Systems", Hemisphere Publishing Corp., New York (1982).

3. VAN DER WELLE, R., "Void Fraction, Bubble Velocity and Bubble Size in Two-Phase Flow", *Int. J. Multiphase Flow* 11(3):317-345 (1985).

4. CHEREMISINOFF, N.P., "Measurement Techniques for Multiphase Flows", Encyclopedia of Fluid Mechanics Volume 1 - Flow Phenomena and Measurement, N.P. Cheremisinoff, Ed., Houston, Gulf Publishing Company, 1280-1338 (1986).

5. SAXENA, S.C., PATEL, D., SMITH, D.N., and RUETHER, J.A., "An Assessment of Experimental Techniques for the Measurement of Bubble Size in a Bubble Slurry Reactor as Applied to Indirect Coal Liquefaction", *Chem. Eng. Commun.* 63:87-127 (1988).

6. SHOOK, C.A., and ROCO, M.C., "Slurry Flow: Principles and Practice", Butterworth-Heinemann, Boston (1991).

7. WALMSLEY, M.R.W., "Air Bubble Motion in Wood Pulp Fibre Suspension", APPITA 1992 Proceedings, 509-515 (1992).

8. HUNOLD, M., KRAUTHAUF, T., MÜLLER, J., and PUTZ, H.-J., "Effect of Air Volume and Air Bubble Size Distribution on Flotation in Injector Aerated Deinking Cells", *J. Pulp Paper Sci.* 23(12):J555-560 (1997).

9. JULIEN SAINT AMAND, F., "Hydrodynamics of Flotation: Experimental Studies and Theoretical Analysis", 1997 TAPPI Recycling Symposium, Atlanta, GA, TAPPI Press, 219-241 (1997).

10. PRIMEX PHYSICS INTERNATIONAL, "Flash X-ray Seminar", San Leandro, CA (1996).

11. JAMET, F., and THOMER, G., "Flash Radiography", Elsevier Publishing Company, Inc., New York (1976).

12. CARTZ, L., "Nondestructive Testing", ASM International, Materials Park, OH (1995).

13. BENNETT, A.W., HEWITT, G.F., KEARSEY, H.A., KEEYS, R.K.F., and LACEY, P.M.C., "Flow Visualization Studies of Boiling at High Pressure", *Proc. Inst. Mech. Eng.* 180:1-11 (1965).

14. HEWITT, G.F., and ROBERTS, D.N., "Studies of Two-Phase Flow Patterns by Simultaneous X-ray and Flash Photography", United Kingdom Atomic Energy Authority (UKAEA), Harwell, Berkshire, Report Number: AERE-M2159 (1969).

15. ROWE, P.N., and PARTRIDGE, B.A., "An X-ray Study of Bubbles in Fluidised Beds", *Trans. Inst. Chem. Eng.* 43:T157-175 (1965).

16. FARRINGTON, T.E., JR., "A More Fundamental Approach to the Problem of High Consistency Forming", 1986 TAPPI Engineering Conference, Atlanta, GA, TAPPI Press, 709-717 (1986).

17. FARRINGTON, T.E., JR., "Soft X-ray Imaging Can Be Used To Assess Sheet Formation and Quality", *TAPPI J.* 71(5):140-144 (1988).

18. FARRINGTON, T.E., JR., "Flash X-ray Imaging of Kraft Black Liquor Sprays", *TAPPI J.* 71(2):89-92 (1988).

19. TRIANTAFILLOPOULOS, N.G., and FARRINGTON, T.E., JR., "Flash X-ray Radiography Techniques for Visualizing Coating Flows", 1988 TAPPI Coating Conference, New Orleans, LA, TAPPI Press, 47-52 (1988).

20. ZAVAGLIA, J.C., and LINDSAY, J.D., "Flash X-ray Visualization of Multiphase Flow During Impulse Drying", *TAPPI J.* 72(9):79-85 (1989).

21. HEINDEL, T.J., and MONEFELDT, J.L., "Flash X-ray Radiography for Visualizing Gas Flows in Opaque Liquid/Fiber Suspensions", 6th International Symposium on Gas-Liquid Two-Phase Flows, Vancouver, BC, ASME Press (June 22-26, 1997).

22. HEINDEL, T.J., and MONEFELDT, J.L., "Observations of the Bubble Dynamics in a Pulp Suspension Using Flash X-ray Radiography", 1997 TAPPI Engineering & Paper Makers Super Conference, Atlanta, GA, TAPPI Press, 1421-1427 (1997).

23. MONEFELDT, J.L., "Flow Structures in a Quiescent Rectangular Bubble Column", Masters Thesis, Institute of Paper Science and Technology, Atlanta, GA (1996).

24. TAPPI, "T 205 om-88 - Forming Handsheets for Physical Tests of Pulp", TAPPI Test Methods 1994-1995, Atlanta, TAPPI Press (1994).

25. STENUF, T.J., and UNBEHEND, J.E., "Hydrodynamics of Fiber Suspensions", Encyclopedia of Fluid Mechanics: Vol. 5 - Slurry Flow Technology, N.P. Cheremisinoff, Ed., Houston, Gulf Publishing Company, 291-308 (1986).

26. KEREKES, R.J., SOSZYNSKI, R.M., and TAM DOO, P.A., "The Flocculation of Pulp Fibres", Papermaking Raw Materials, V. Punton, Ed., London, Mechanical Engineering Publications Limited, 265-310 (1985).

27. IGUCHI, M., KAWAJIRI, A., TOMIDA, H., and MORITA, Z., "Effects of the Viscosity of Liquid on the Characteristics of Vertical Bubbling Jet in a Cylindrical Vessel", *ISIJ Int.* 33(3):361-368 (1993).

TABLES

Table 1: Average equivalent bubble diameter and Sauter mean bubble diameter in various consistency fiber suspensions with two different air injection techniques.

	Septum			Sparger		
Consistency	Average Diameter (mm)	Standard Deviation (mm)	Sauter Mean Diameter (mm)	Average Diameter (mm)	Standard Deviation (mm)	Sauter Mean Diameter (mm)
0%	2.9	1.0	3.6	2.0	0.7	2.6
0.1%	3.1	1.0	3.6	2.3	0.8	2.9
0.5%	3.0	1.0	3.6	3.5	1.0	4.2
1.0%	3.4	1.1	4.1	3.6	1.4	4.7

LIST OF FIGURES

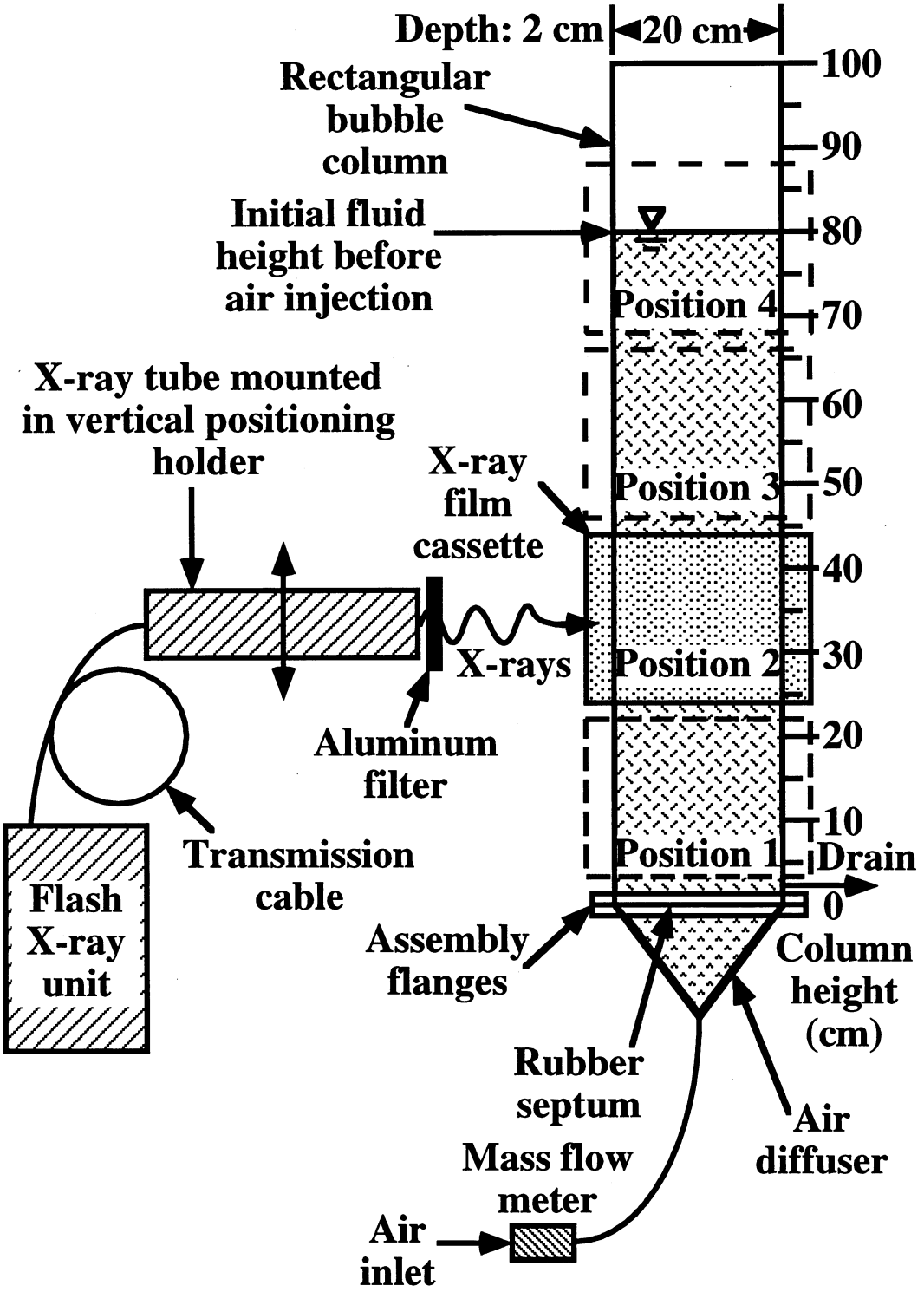
Depth: 2 cm
20 cm
Rectangular bubble column
Initial fluid height before air injection
X-ray tube mounted in vertical positioning holder
X-ray film cassette
X-rays
Aluminum filter
Transmission cable
Flash X-ray unit
Position 4
Position 3
Position 2
Position 1
Drain
Assembly flanges
Rubber septum
Mass flow meter
Air inlet
Air diffuser
Column height (cm)
100
90
80
70
60
50
40
30
20
10
0

Figure 1

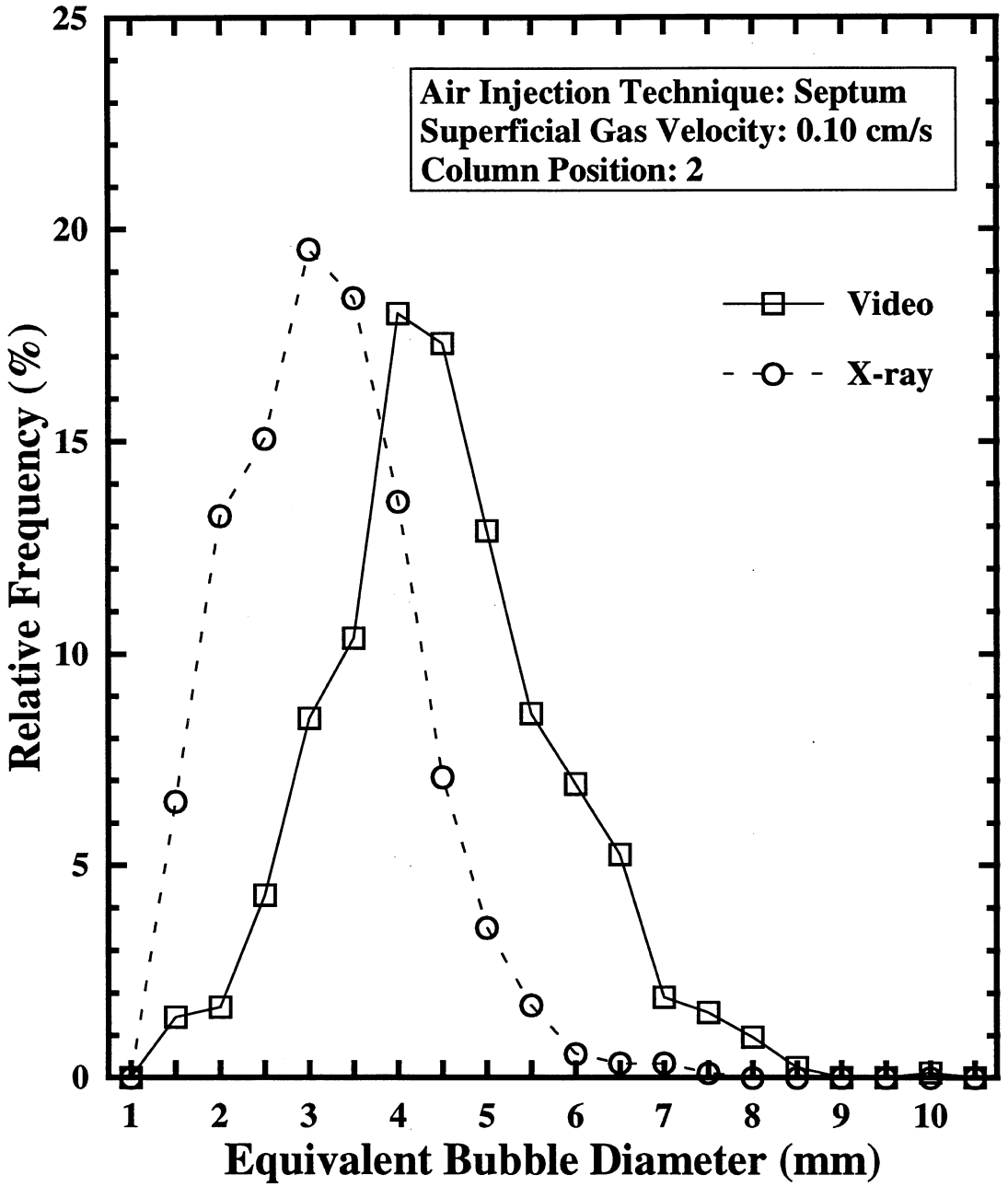
Air Injection Technique: Septum
Superficial Gas Velocity: 0.10 cm/s
Column Position: 2
Video
X-ray
Relative Frequency (%)
Equivalent Bubble Diameter (mm)
0
5
10
15
20
25
1
2
3
4
5
6
7
8
9
10

Figure 2

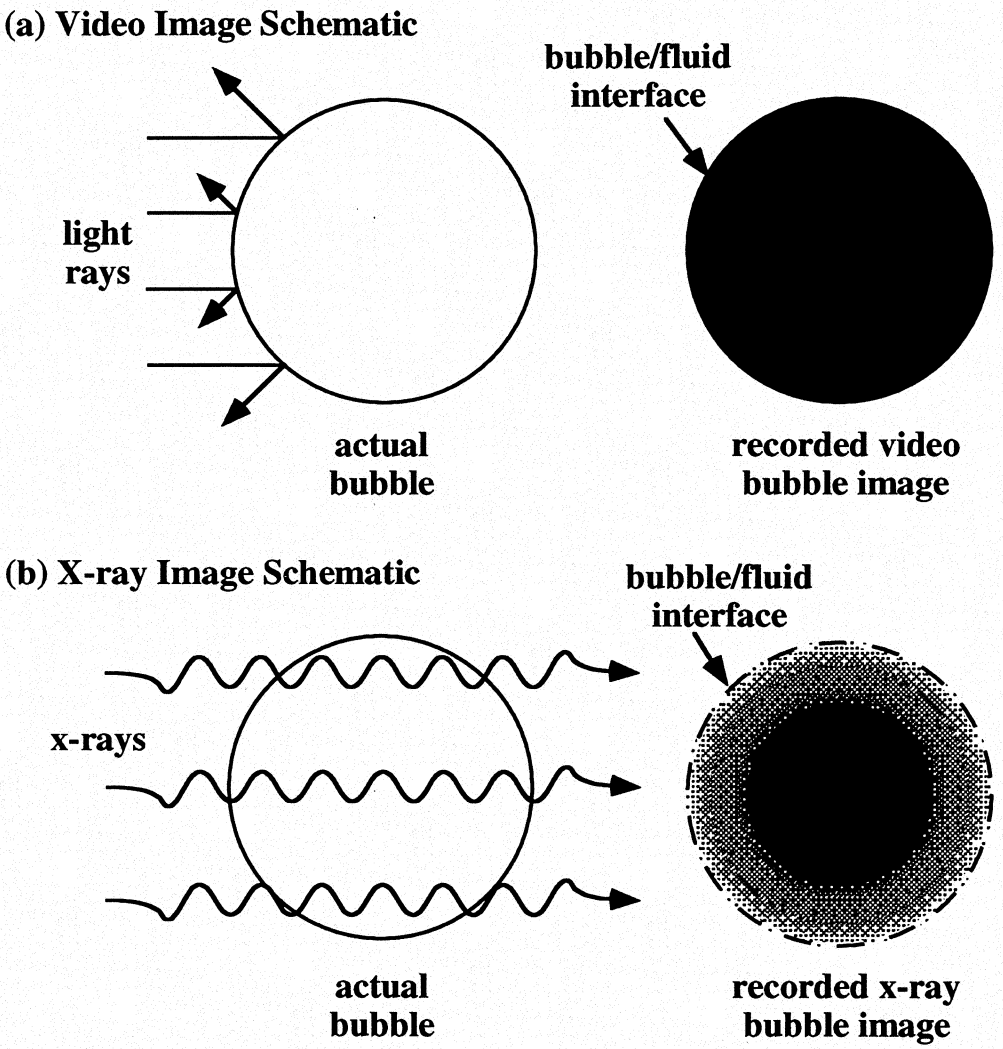
(a) Video Image Schematic
bubble/fluid interface
light rays
actual bubble
recorded video bubble image
(b) X-ray Image Schematic
bubble/fluid interface
x-rays
actual bubble
recorded x-ray bubble image

Figure 3

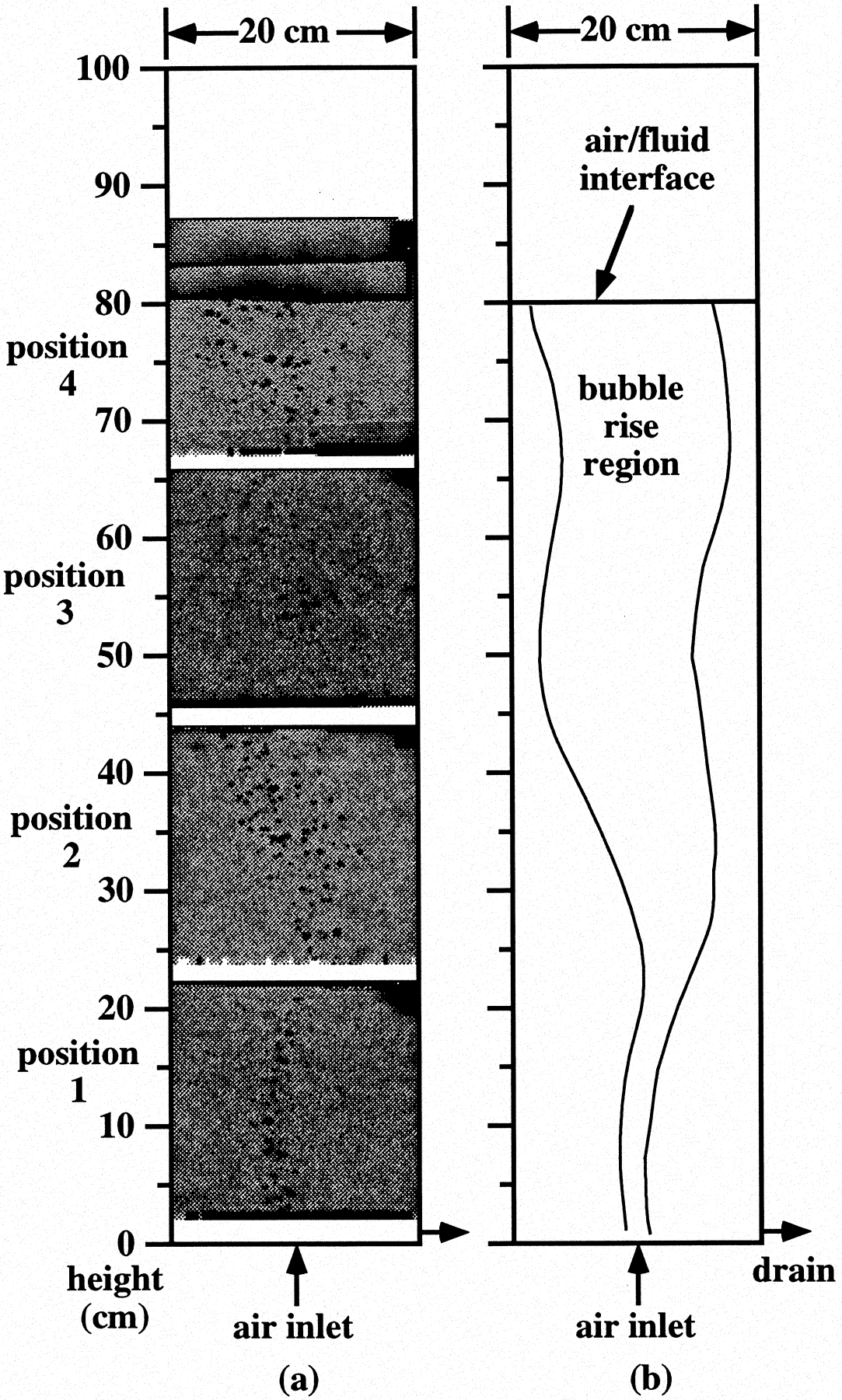
20 cm
20 cm
100
90
80
position
4
70
60
position
3
50
40
position
2
30
20
position
1
10
0
height
(cm)
air inlet
(a)
air/fluid
interface
bubble
rise
region
drain
air inlet
(b)

Figure 4

(a) Air/water system x-ray

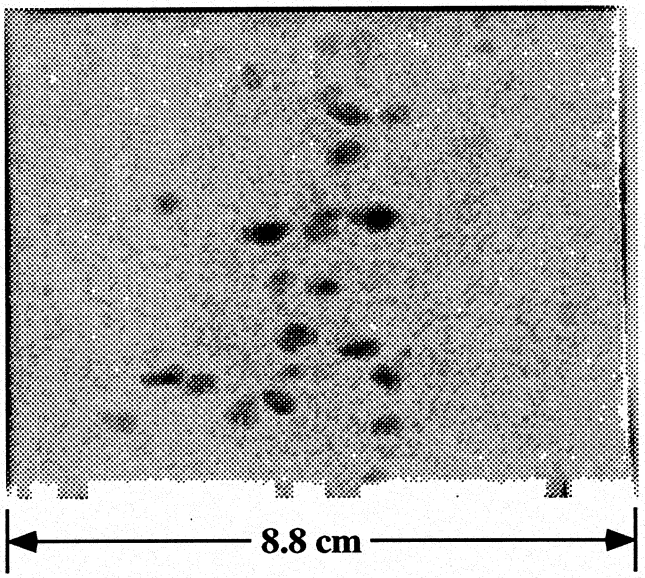

(b) Air/water system x-ray bubble outline

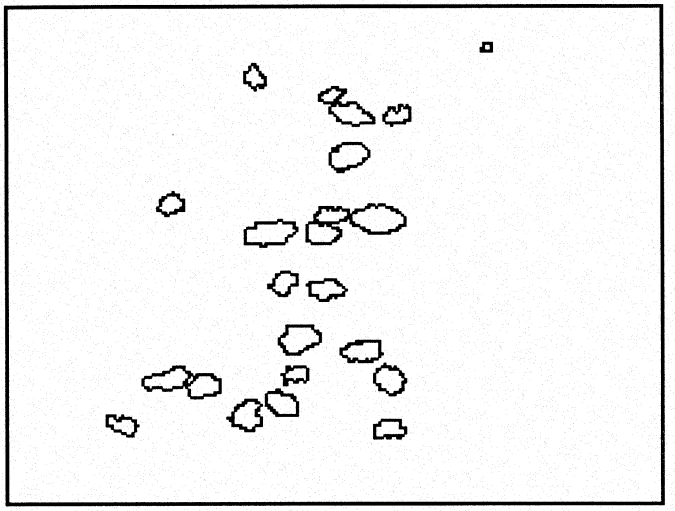

(c) Air/water/0.1% ONP system

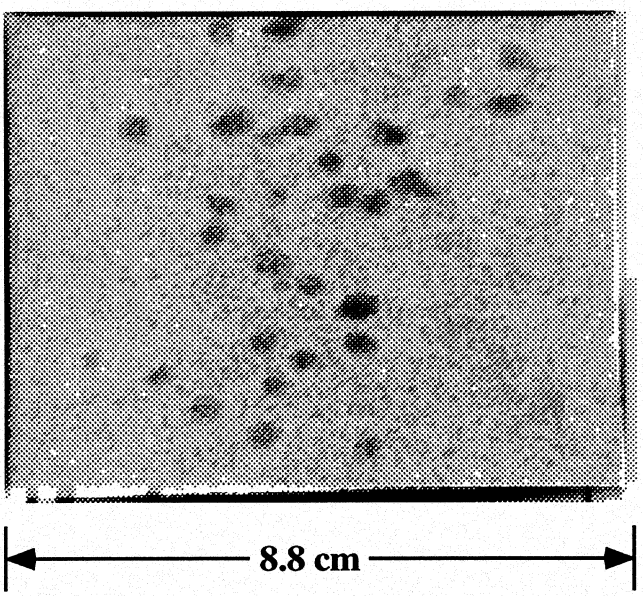

(d) Air/water/0.1% system x-ray bubble outline

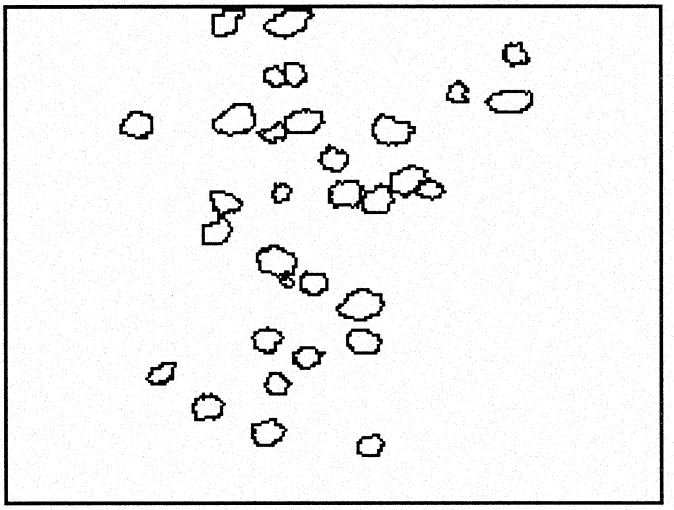

Figure 5

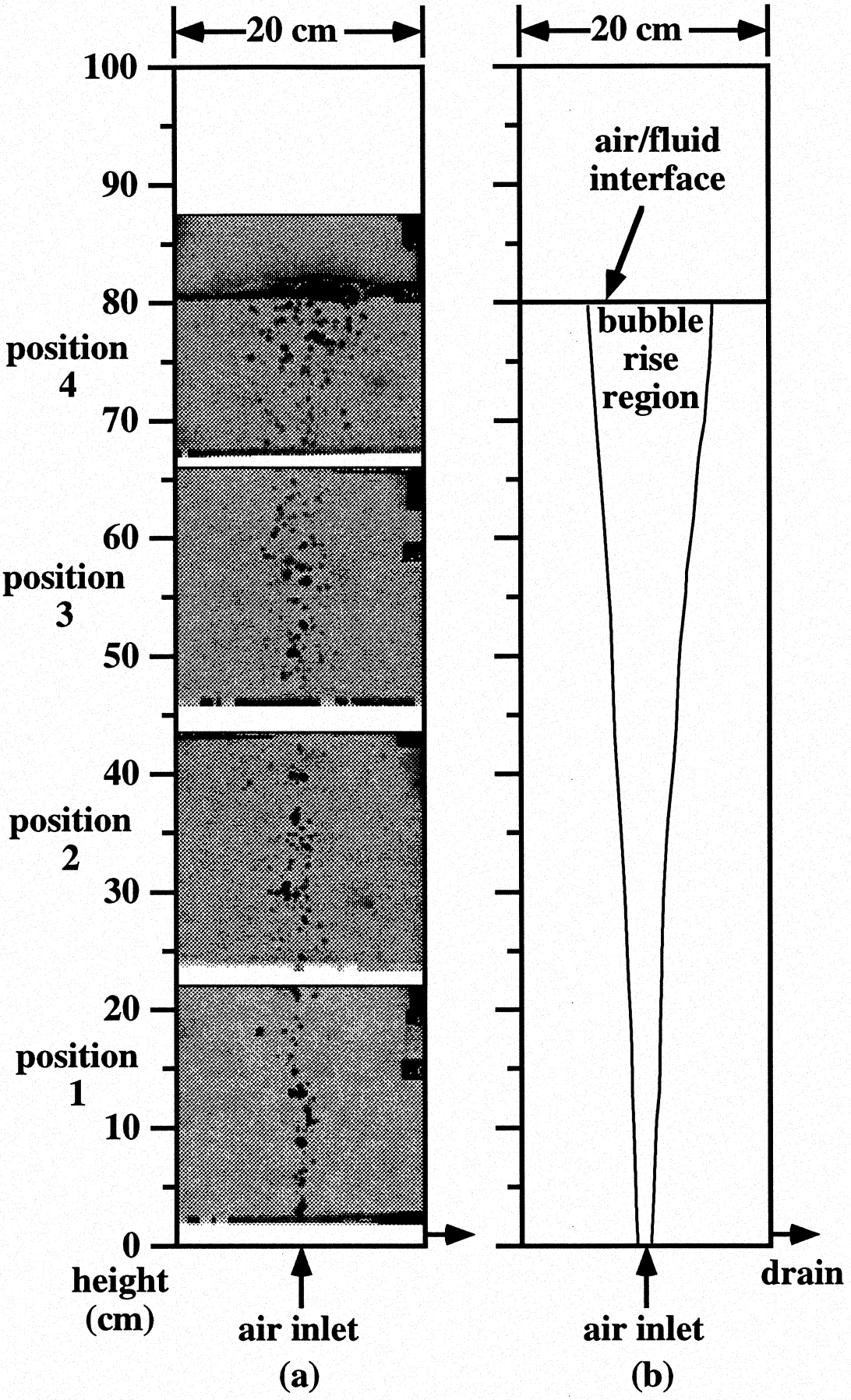
20 cm
20 cm
100
90
80
position 4
70
60
position 3
50
40
position 2
30
20
position 1
10
0
height (cm)
air inlet
(a)
air/fluid interface
bubble rise region
drain
air inlet
(b)

Figure 6

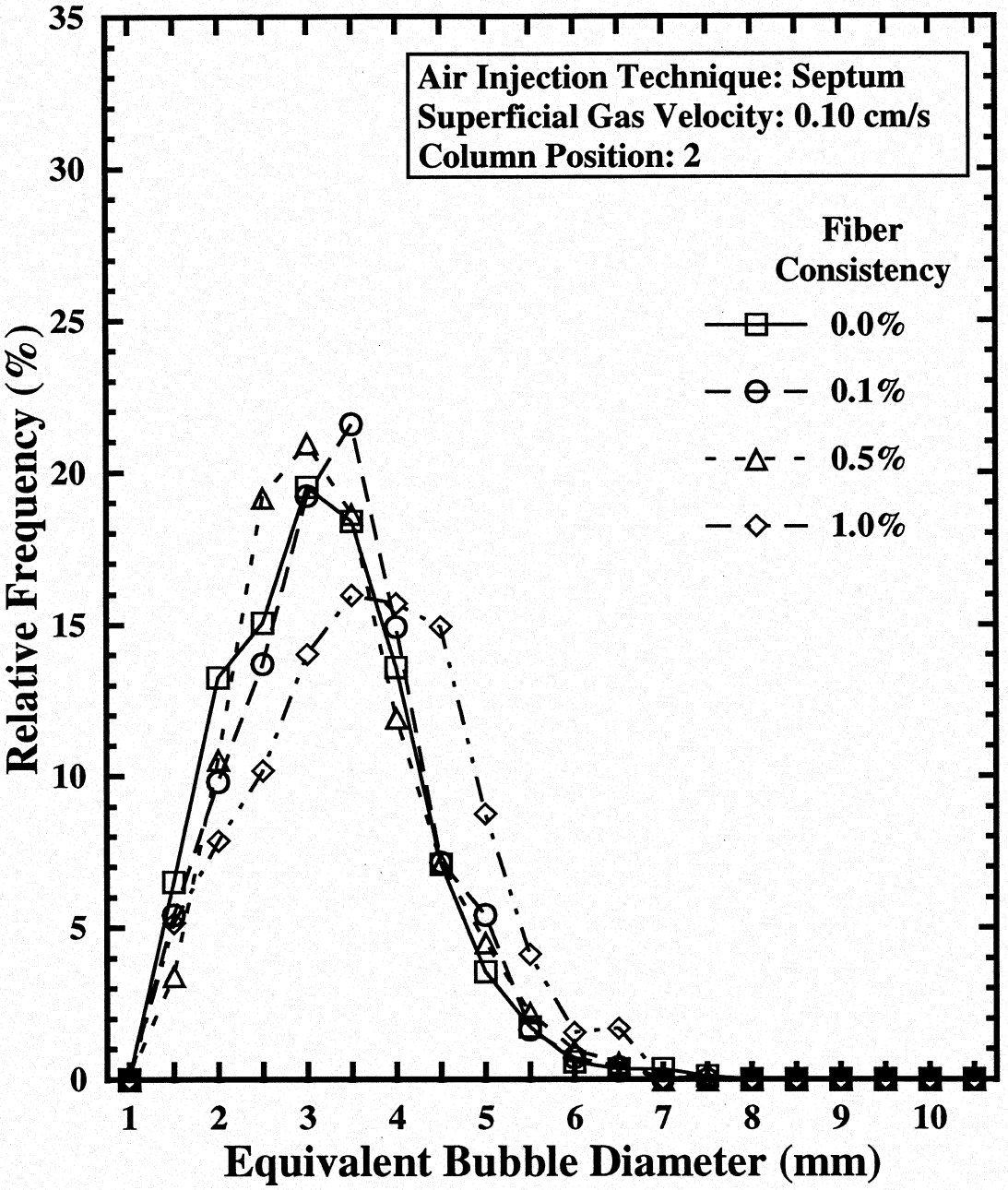
Air Injection Technique: Septum
Superficial Gas Velocity: 0.10 cm/s
Column Position: 2
Fiber Consistency
0.0%
0.1%
0.5%
1.0%
Relative Frequency (%)
Equivalent Bubble Diameter (mm)
0
5
10
15
20
25
30
35
1
2
3
4
5
6
7
8
9
10

Figure 7

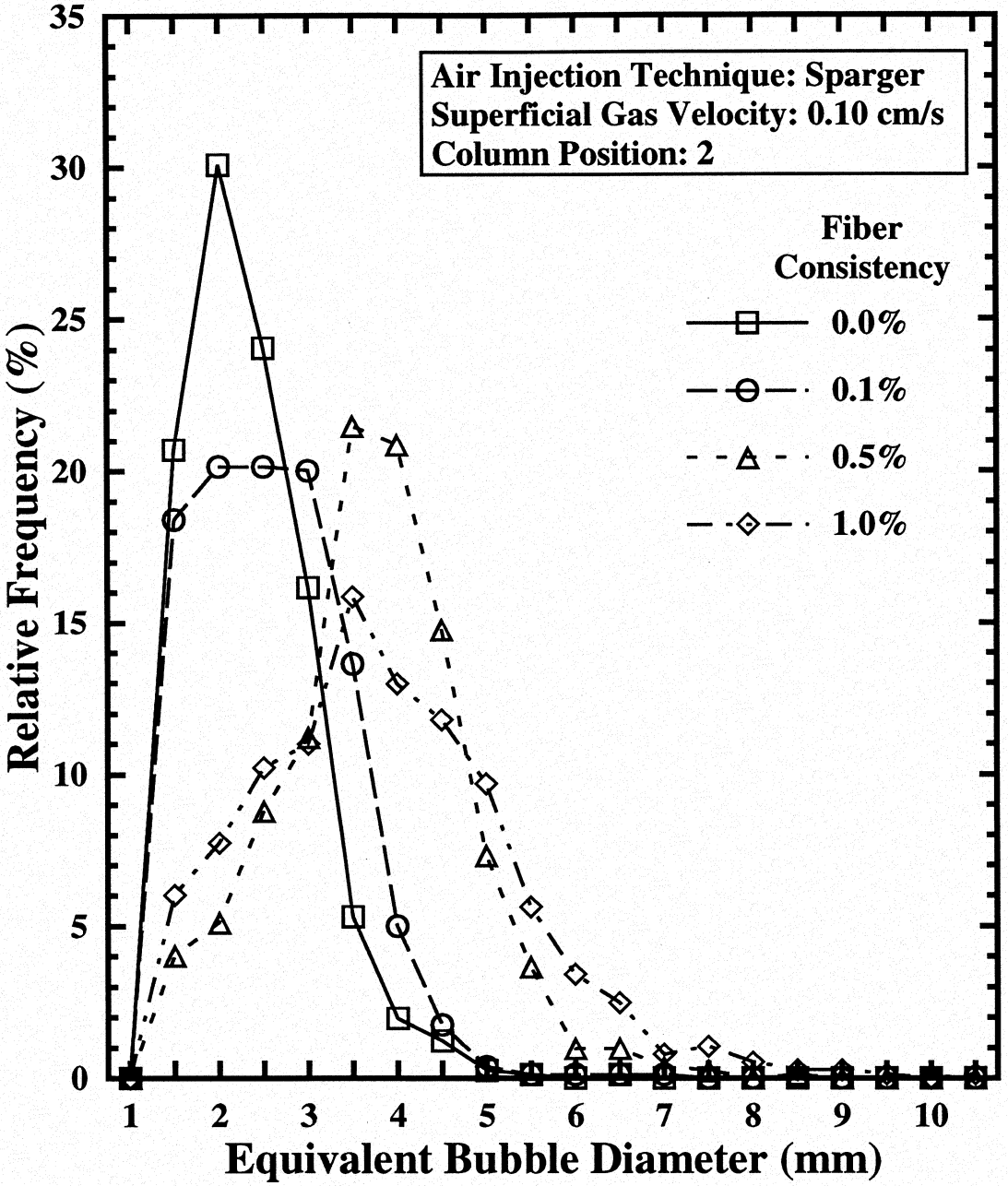
Air Injection Technique: Sparger
Superficial Gas Velocity: 0.10 cm/s
Column Position: 2
Fiber Consistency
0.0%
0.1%
0.5%
1.0%
Relative Frequency (%)
Equivalent Bubble Diameter (mm)
0
5
10
15
20
25
30
35
1
2
3
4
5
6
7
8
9
10

Figure 8

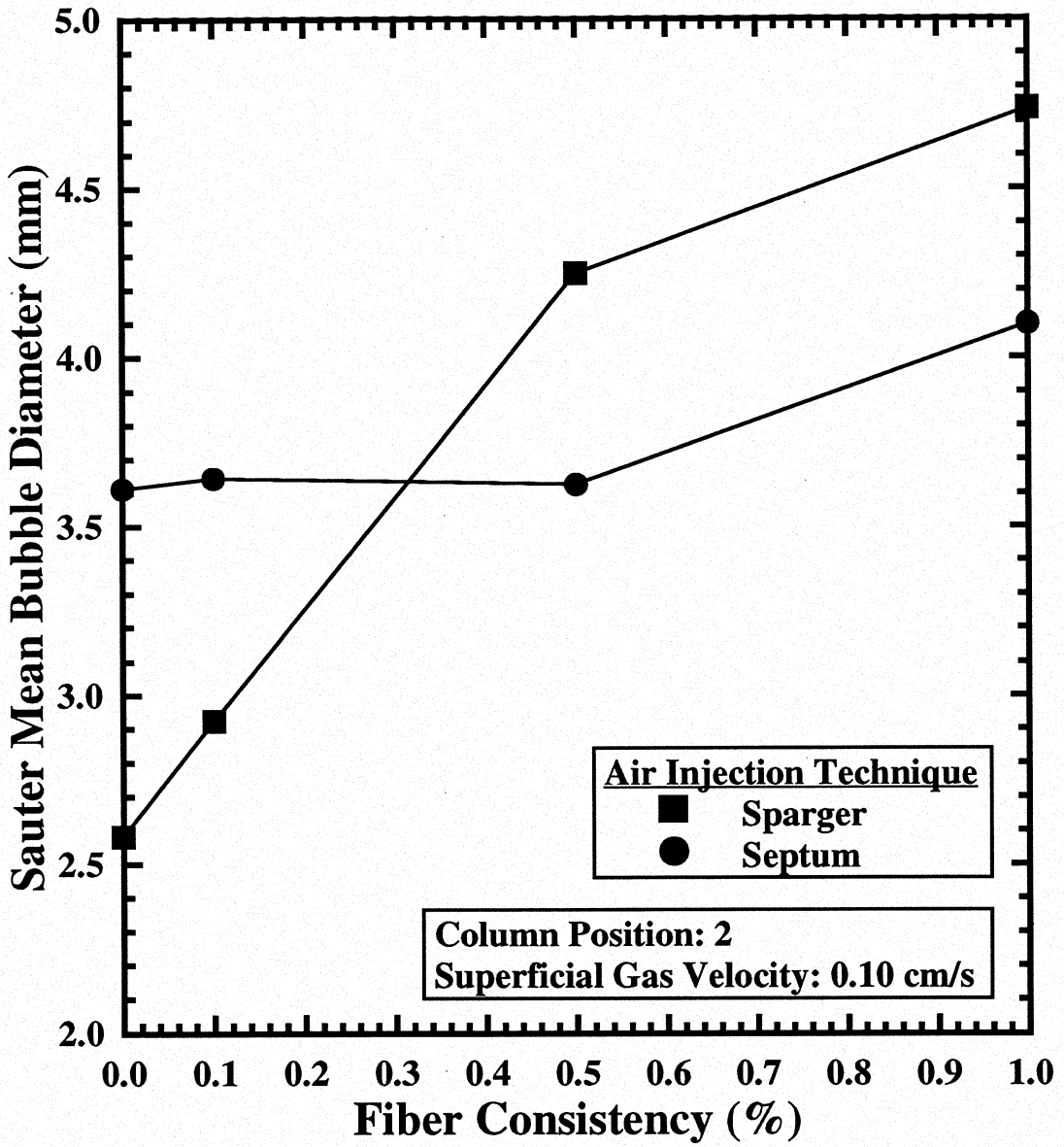
5.0
4.5
4.0
3.5
3.0
2.5
2.0
Sauter Mean Bubble Diameter (mm)
0.0
0.1
0.2
0.3
0.4
0.5
0.6
0.7
0.8
0.9
1.0
Fiber Consistency (%)
Air Injection Technique
Sparger
Septum
Column Position: 2
Superficial Gas Velocity: 0.10 cm/s

Figure 9